Electrochemical Filtering of CO from Fuel-Cell Reformate

Balasubramanian Lakshmanan
University of South Carolina - Columbia

Wayne Huang

John W. Weidner
University of South Carolina - Columbia, weidner@engr.sc.edu

Publication Info

Electrochemical Filtering of CO from Fuel-Cell Reformate

Balasubramanian Lakshmanan,[a,*] **Wayne Huang,**[b] **and John W. Weidner**[a,**,z]

[a]*Center for Electrochemical Engineering, Department of Chemical Engineering, University of South Carolina, Columbia, South Carolina 29208, USA*
[b]*Plug Power Incorporated, Latham, New York 12110, USA*

A proton exchange membrane fuel cell was used as a flow reactor for continuous preferential oxidation of CO over H_2 from 1.0% CO in H_2 under pulse-potential control. By varying the pulse profile (*e.g.*, on-time, off-time, pulse potential) the CO and H_2 oxidation currents were varied independently. The improvement in faradaic selectivity between CO and H_2 oxidation results from the promotion of CO adsorption during the off (*i.e.*, open-circuit) portion of the pulse. Therefore, during the on portion CO oxidation was preferred while the surface was covered with CO.
© 2002 The Electrochemical Society. [DOI: 10.1149/1.1516411] All rights reserved.

Proton exchange membrane fuel cells (PEMFC) operating on pure hydrogen show good polarization characteristics over a wide range of load and temperature conditions. However, using pure H_2 as a fuel in automotive and residential applications has many limitations. The infrastructure to deliver H_2 is inadequate, the refueling of gaseous H_2 can be slow, and the storage of H_2 is problematic.[1] Hence, using an onboard reformer to produce a H_2-rich stream from fuels like natural gas, gasoline, and methanol is gaining popularity.[2] The gas from the reformer, commonly called reformate, is a mixture of nitrogen (40-50%), hydrogen (35-45%), CO_2 (10-20%), CO, water vapor, and traces of other gases. The CO content of the unscrubbed reformate is typically greater than 10 mol % (100,000 ppm).[3] Such high concentrations of CO in the fuel render the PEMFC inoperable due to the poisoning of the anode catalysts.[4-7]

To lower the CO content of a fuel, multiple stages of CO cleanup are required to process the gas from the reformer. Figure 1a shows a block diagram of a conventional fuel processing system, consisting of a high temperature shift (HTS) and a low temperature shift (LTS) reactor to convert CO into H_2 using the water gas shift reaction. The fuel exiting the LTS is then fed to a preferential partial oxidizer (PrOx), wherein the CO concentration is lowered to the level acceptable to fuel cells (~50 ppm CO) by oxidation of CO with air to form CO_2. The approximate CO concentrations fed to each of these reactor units are given in the figure. Each block shown in the figure is drawn to the relative size of the units in a typical commercial system. Therefore, the total volume of the cleanup stages is more than one order of magnitude larger than the reformer and the fuel cell stack combined.[8,9] Another limitation of the cleanup stages in a conventional gas processing system is the poor selectivity of the PrOx reactor for oxidizing CO over H_2. The typical selectivity of a PrOx toward CO oxidation is less than 1:10 (ten times more H_2 is oxidized than CO) resulting in a consumption of close to 1.0% of the H_2 produced in the reformer and the water gas shift reactors.[10,11]

Here we demonstrate a method by which one or more stages of CO cleanup in a fuel processing system may be replaced. Namely, an electrochemical filter (EF) for CO using current PEMFC technology that preferentially oxidizes CO over H_2 in reformate. The configuration of the proposed fuel processing system is shown in Fig. 1b. The proposed filter may be capable of replacing either the LTS, PrOx reactor, or both LTS and PrOx reactors used in a conventional fuel processing system.

The electrochemical filter operated under a pulse potential mode to achieve high selectivity for CO oxidation over H_2 oxidation. During the off portion of the pulse, the cell is open-circuited and CO adsorption was promoted. During the on portion, CO oxidation was

preferred over H_2 oxidation while the surface was covered with CO. Repeated pulsing enables continuous removal of CO from the reformate. Hydrogen is produced on the cathode from H^+ formed during the oxidation of CO and H_2, such that the overall reactions in the cell are given by Reactions 1 and 2.

$$CO + H_2O \rightarrow H_2 + CO_2 \qquad [1]$$

$$H_2 \rightarrow H_2 \qquad [2]$$

Reaction 2 is shown to remind us that all the H_2 oxidized at the anode is formed back in the cathode resulting in no net consumption of H_2. However, this reaction does represent a net power consumption in the device thus impacting the overall electrical efficiency of the fuel cell system. Thus the selectivity reported here is a measure of electrochemical efficiency rather than direct fuel consumption. This is in contrast to a PrOx reactor, which involves competitive oxidation of CO and H_2 by reaction with air to form CO_2 and H_2O, respectively. Here we show that by using a standard fuel cell cata-

a) Conventional Fuel Processing System
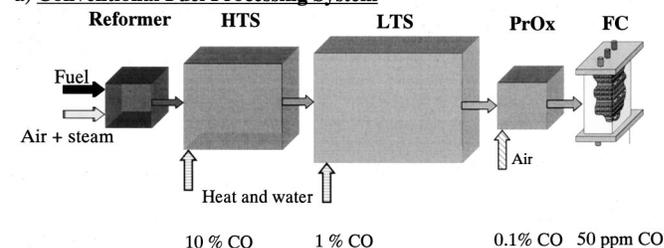
b) Proposed Fuel Processing System
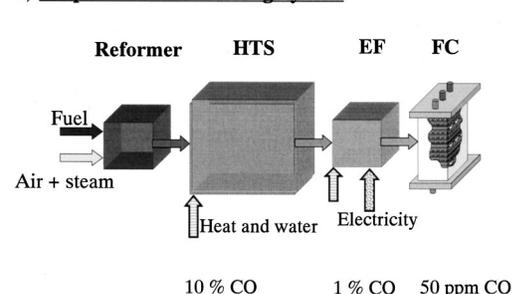
Figure 1. Block diagram of the conventional fuel processing system compared to the proposed fuel processing system. In the latter, the electrochemical filter (EF) for CO replaces the LTS and PrOx. Each block shown in the conventional system is drawn to the relative size of the units in a typical commercial system. The size of the EF unit is the anticipated size of the unit in an optimized device. The average inlet CO composition of each unit is shown in the figure, the balance is H_2, N_2, CO_2, and water.

* Electrochemical Society Student Member.
** Electrochemical Society Active Member.
z E-mail: weidner@engr.sc.edu

lyst, we can affect the amount of CO oxidized and the selectivity of CO over H_2 by varying the applied voltage, on-time, and off-time of the pulse potential profile.

Experimental

Flow cell.—Catalyzed membranes were prepared using a procedure similar to the steps described in U.S. pat. 5,211,984.[12] The active area of the electrodes was 50 cm^2, the anode side had a catalyst loading of 0.45 mg/cm^2 of 1:1 atomic ratio Pt-Ru catalyst, while the cathode was made of 0.5 mg/cm^2 of Pt. The membrane was catalyzed by hot pressing at 140°C under 1000 psig pressure for 2 min against Teflon decals sprayed with catalyst ink. The catalyzed membrane was then bonded to carbon cloth gas-diffusion layers (GDL) at 140°C under 500 psig pressure for 2 min to form a membrane electrode assembly (MEA). The MEA was assembled into a fuel cell with single-channel serpentine flow field plates bought from Fuel Cell Technologies. The cathode side had H_2 flowing at 0.05 standard liters per minute (slm). The cathode side was used as the counter and reference electrode (*i.e.*, dynamic hydrogen electrode, DHE) such that all the potentials reported here are referred to DHE. The anode side had a flow of either N_2 or 1.0% (10,000 ppm) CO in H_2. All the gases were obtained from Air Products and the concentrations certified by the manufacturer. All the pure gases used were certified ultrahigh purity (UHP). Concentration of CO in hydrogen was verified independently using a Buck Scientific gas chromatograph (GC), model 910, equipped with both thermal conductivity detector (TCD) and flame ionization detector (FID).

Cyclic voltammetry.—For electrochemical characterization of the Pt-Ru MEA, N_2 was first flowed at 0.10 slm through the anode side, and the cell was left at open circuit. The N_2 flow was switched to a flow of 1.0% CO in H_2 with a total flow rate of 0.10 slm for a specified period of time (referred as exposure time) after which N_2 flow was restored. The cell was held at a constant potential of 50 mV for 15 s, which was followed by cyclic voltammetry (CV) at a scan rate of 10 mV/s from 50 to 1000 mV and back to 50 mV. Experiments were conducted using an M263A potentiostat/galvanostat and ECHEM software made by EG&G. The area under the CO oxidation peak relative to the background current was used to calculate the amount of CO oxidized, which is reported as the amount of CO adsorbed. The CV area relative to the background was checked at other scan rates to confirm that no appreciable chemical desorption was occurring during the oxidation step. The experiment was repeated for various durations of CO in H_2 exposure. Between each experiment, another CV was performed on the electrode and the resulting voltammogram overlapped with the background, confirming that all adsorbed CO was oxidized in the first cycle.

Pulse potential.—To study the amount of CO and H_2 oxidized by the filter, N_2 flow on the anode side was switched to a flow of 1.0% CO in H_2 at a total flow rate of 0.10 slm. The flow rate of 0.10 slm corresponds to a space velocity of 1200/h based on the flow channel volume, and this space velocity corresponds to the typical space velocity used in LTS reactor. The electrode was polarized to a desired potential during the on portion of the pulse and open-circuited during the off portion of the pulse. The pulse profile was applied for 25 min. The outlet gas from the anode was collected using a sampling bag (200 mL) during the final 5 min. The gas from the sampling bag was injected into the GC with a TCD and FID for analysis. The use of sampling bags provided an average concentration of the gases and helped to improve the consistency of the analyses. The concentrations of the gases reported here are an average of at least three analyses from the GC. The inlet molar flow rate to the anode, f^0, was controlled using a digital mass flow controller. The change in the mole fractions of CO and CO_2 between the inlet and the outlet was used to calculate the outlet flow rate from the anode, f, using
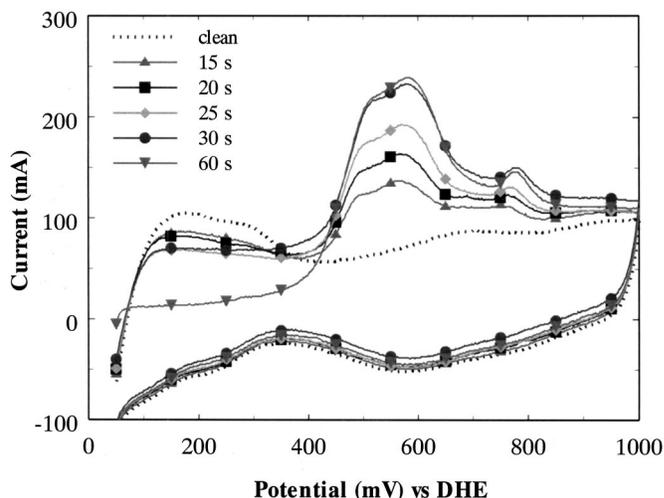
Figure 2. Cyclic voltammetry on a Pt-Ru composite electrode in N_2 flow after various exposure times to 1.0% CO in H_2. The total flow rate was 0.10 slm. The dotted line corresponds to a clean electrode while the symbols correspond to time duration of CO exposure indicated by the legend.

$$f = f^0 \frac{x_{CO}^0}{x_{CO} + x_{CO_2}} \quad [3]$$

where x_i^0 and x_i (i refers to either CO, CO_2, or H_2) are the mole fractions of each species in the inlet and outlet streams, respectively. The reaction rates of each species, r_i, and the faradaic current, i_i, going into each reaction is calculated from Eq. 4 and 5, respectively

$$r_i = f^0 x_i^0 - f x_i \quad [4]$$

$$i_i = 2 F r_i \quad [5]$$

where F is the Faraday constant. The selectivity (*i.e.*, the fraction of faradaic current going to CO oxidation) is defined by

$$\text{Selectivity} = \frac{i_{CO}}{i_{CO} + i_{H_2}} \quad [6]$$

Results and Discussion

Figure 2 contains the CVs in N_2 on Pt-Ru catalysts after exposure to 1.0% CO in H_2. The dotted line corresponds to a clean electrode while the symbols correspond to different durations of CO exposure. The cell was open-circuited during CO exposure. In this figure, the current between 60 and 300 mV in the forward scan corresponds to the oxidation of adsorbed hydrogen. The oxidation of CO starts at potentials more positive than 350 mV and reaches a maximum rate at approximately 600 mV. Electro-oxidation of CO occurs through

$$CO + H_2O \rightarrow CO_2 + 2H^+ + e^- \quad [7]$$

The mechanistic steps for this reaction are (M refers to either Pt or Ru metal catalysts sites)

$$M + CO \rightleftarrows M\text{-}CO \quad [8]$$

$$M + H_2O \rightleftarrows M\text{-}OH + H^+ + e^- \quad [9]$$

$$M\text{-}CO + M\text{-}OH \rightarrow 2M + CO_2 + H^+ + e^- \quad [10]$$

Reaction 8 corresponds to the adsorption of CO onto the Pt-Ru catalyst (*i.e.*, CO poisoning). Reaction 9 corresponds to the formation of hydroxyl ions via oxidation of water, and Reaction 10 cor-
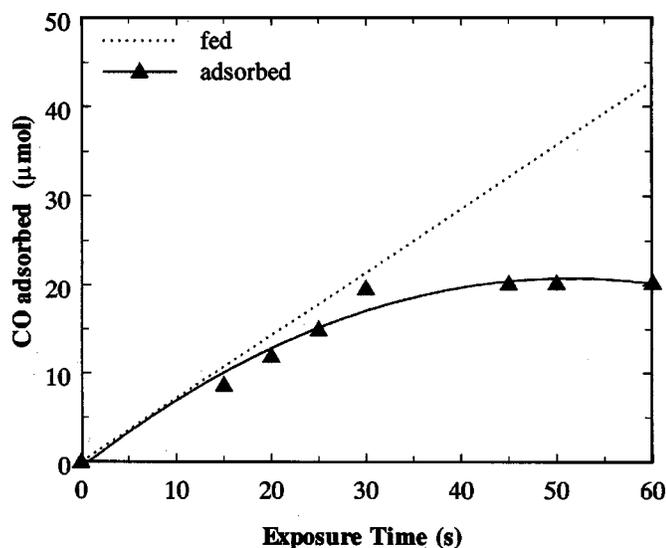
Figure 3. The amount of CO adsorbed on a Pt-Ru electrode *vs.* the exposure time. The dotted line is the amount of CO fed during this time. The feed was 1.0% CO in H_2 at 0.10 slm.

responds to the oxidation of adsorbed CO by reaction with the hydroxyl species.[13-16] The competitive adsorption and oxidation of H_2 are shown in Reactions 11 and 12, respectively

$$2M + H_2 \rightleftarrows 2M\text{-}H \qquad [11]$$

$$M\text{-}H \rightleftarrows M + H^+ + e^- \qquad [12]$$
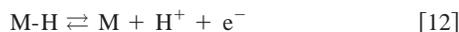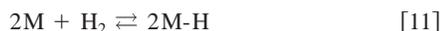
Integrating the area under the CV between 350 and 1000 mV shown in Fig. 2, and correcting it for the background area, gives the amount of CO adsorbed during the exposure time. The amount of CO adsorbed as a function of exposure time is plotted as symbols in Fig. 3 (the solid line is a line of best fit through the data). The dotted line is the cumulative amount of CO fed. At short times (<15 s), most of the CO fed is adsorbed and the solid line overlaps with the dotted line. At longer times, the CO coverage on the catalyst material increases until all the catalyst sites are filled with CO, resulting in saturated coverage. For example, only 66% of the CO fed was adsorbed when the flow was on for 45 s. Higher exposure times do show no significant increase in CO adsorption, which leads to more CO in the outlet. Therefore, for 1.0% CO in H_2 flowing at 0.10 slm, a clean electrode is saturated in 45 s. This is set as the upper limit for the off-time in the pulse profile.

The lower limit for the on-time is determined by the RC (*i.e.*, resistance × capacitance) time constant of the catalyst layer. On-times less than one RC time constant result in most of the coulombs going into charging the double layer rather than the desired faradaic reaction. For the carbon-supported catalyst used here, an RC time constant of approximately 2.3 s was obtained from a potential step in N_2.

Using 45 s as the upper limit for the off-time and 2 s as the lower limit for on-time, the performance of the CO filter was studied at 0.6 and 1.0 V as a function of duty cycle (ratio of on-time to total time). Figures 4a and b show the fraction of the inlet CO that reacts and the selectivity between CO and H_2 oxidation, respectively. For the three sets of conditions shown in Fig. 4a, the rate of CO oxidation increases with duty cycle. As the duty cycle is increased, a larger fraction of the time is spent oxidizing CO and hence more CO is oxidized to CO_2. However, H_2 oxidation also increases with increasing on-time. The change in selectivity depends on which reaction is more sensitive to a change in the on-time. For example, at 1.0 V, H_2 oxidation increases faster than CO oxidation and hence the selectivity shown in Fig. 4b decreases with increasing duty cycle. At

(a)   **Duty Cycle** $= t_{on}/(t_{on}+t_{off})$

(b)   **Duty Cycle** $= t_{on}/(t_{on}+t_{off})$
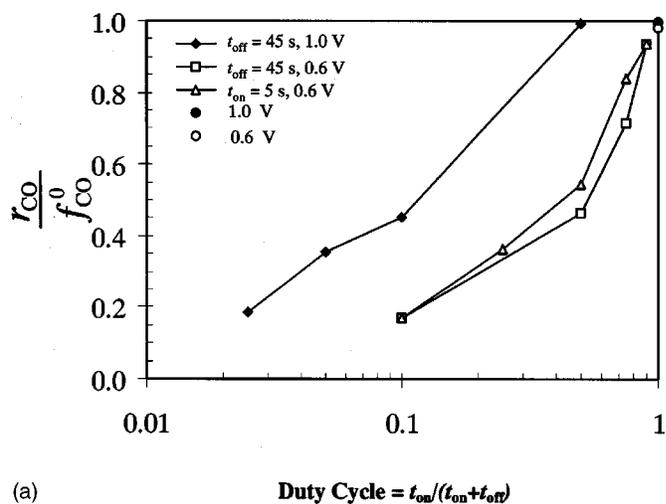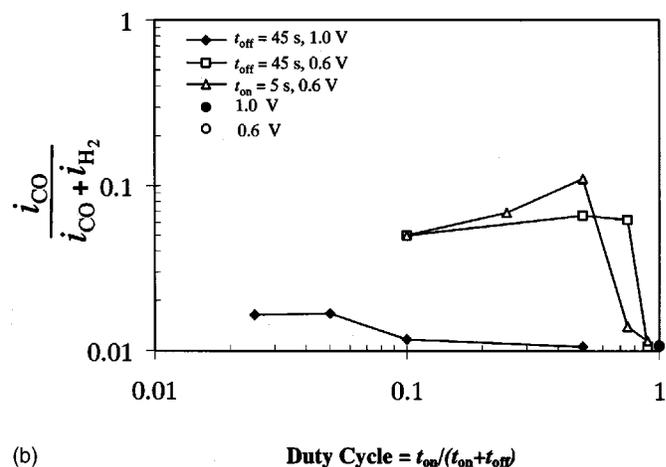
Figure 4. (a) The rate of CO reaction over the rate of CO fed as function of duty cycle [(♦) t_{off} = 45 s, 1.0 V; (□) t_{off} = 45 s, 0.6 V; (△) t_{on} = 5 s, 0.6 V; (●) constant potential, 1.0 V; and (○) constant potential, 0.6 V]. The experiments were conducted at room temperature with 1.0% CO in H_2 at a total flow rate of 0.10 slm (*i.e.*, f_{CO}^0 = 68.1 µmol/s) on Pt-Ru electrode. (b) The fraction of faradaic current going into the CO oxidation as function of duty cycle [(♦) t_{off} = 45 s, 1.0 V; (□) t_{off} = 45 s, 0.6 V; (△) t_{on} = 5 s, 0.6 V; (●) constant potential, 1.0 V; and (○) constant potential, 0.6 V]. The experiments were conducted at room temperature with 1.0% CO in H_2 at a total flow rate of 0.10 slm (*i.e.*, f_{CO}^0 = 68.1 µmol/s) on Pt-Ru electrode.

duty cycles greater than 0.1, the selectivity approaches the mole fraction of CO in the feed (*i.e.*, 0.01). At duty cycles greater than 0.5, near complete removal of CO is obtained such that the EF device has changed the CO concentration of the feed from 1.0% to 80 ppm while increasing the H_2 molar flow rate by 1.0% (see Reactions 1 and 2). Unfortunately, the dramatically cleaner fuel came at the expense of an extremely low selectivity of 0.011. The EF device acted as an electrochemical pump in which most of the H_2 fuel went from the anode to the cathode at 1.0 V. Even if the FC could deliver its power at 1.0 V and there was no nonfaradaic current, the overall system (EF plus FC) would consume as much power as it produced.

Decreasing the pulse voltage to 0.6 V improved the selectivity of CO oxidation over that of H_2, thus increasing the electrical efficiency of the overall system. For example, at an off-time of 45 s and a duty cycle of 0.1, decreasing the voltage from 1.0 to 0.6 V decreased the H_2 oxidation rate by a factor of 10.8, but decreased the CO oxidation rate by a factor of 2.65 (*i.e.*, the selectivity increased

from 0.012 to 0.050). Therefore, the power consumption of the EF was significantly reduced. However, the CO content of the fuel was only decreased by 17.0%.

Further improvements in both CO oxidation rates and selectivity were achieved by either increasing the duty cycle or decreasing the on-time. For example, at 0.6 V and 45 s off-time, increasing the duty cycle from 0.1 to 0.5 increased CO removal by a factor of 3 while increasing the selectivity by 1.6%. However, further increases in the duty cycle resulted in a drastic drop in selectivity, eventually approaching a value equal to the composition of CO in the feed (0.01). At 0.6 V and a duty cycle of 0.5, decreasing the on-time from 45 to 5 s increased CO removal by 8.0% while increasing the selectivity by a factor of 1.68.

Reducing the on-time to less than 5 s may improve both CO removal and selectivity further. However, the 5 s of on-time is approximately 2 RC time constants for this catalyst layer. Smaller on-times would result in large nonfaradaic currents, thus consuming most of the current during the on portion of the pulse. Further improvements in performance with reduced on-time can be investigated only if the RC time constant of the catalyst layer is reduced.

Conclusions

A PEMFC was used as a flow reactor for continuous preferential oxidation of CO over H_2 from 1.0% CO in H_2 under pulse-potential control. By varying the pulse profile (*e.g.*, on-time, off-time, pulse potential), the CO and H_2 oxidation currents were varied independently. For example, at a constant potential operation of 0.6 V *vs.* DHE, the ratio of the CO to H_2 oxidation currents was in proportion to the fuel composition (*i.e.*, 1:99). Under these conditions, the filter would probably consume more power than a fuel cell could deliver. By continuously pulsing the potential between 0.6 V and open circuit every 5 s, the selectivity of CO oxidation over that of H_2 increased by a factor of 9.25, thus significantly decreasing the power consumed by the device. The CO oxidation rate decreased by only 28%. Improved selectivity between CO and H_2 oxidation results from the promotion of CO adsorption during the off (*i.e.*, open-circuit) portion of the pulse. Therefore, during the on portion CO oxidation is preferred while the surface is covered with CO.

It is anticipated that further improvements in selectivity, CO removal rates, and power consumption are possible by investigating a wider range of pulse profiles as well as other design and operating conditions (*e.g.*, size and composition of the catalyst layer, temperature). To investigate larger off-times than those studied here, without decreasing the flow rate and hence increasing the reactor volume, more catalyst sites per unit volume of the active catalyst layer are needed. This can be done by increasing the catalyst loading either by increasing the weight percent of catalysts or by increasing the cata-

lyst layer thickness. To investigate smaller on-times than those studied here, smaller RC time constants for the catalyst layer are needed. This can be achieved either by decreasing the capacitance of the electrode or by decreasing its resistance. To decrease capacitance, the carbon support should be reduced or eliminated without dramatically decreasing the number of catalysts sites. To decrease the resistance, the cell can be operated at higher temperatures ($\sim80°C$) wherein the ionic conductivity of Nafion is an order of magnitude higher than its room-temperature conductivity. However, the effect of temperature on other variables (*e.g.*, adsorption/desorption, and oxidation rates, capacitance) makes it difficult to speculate whether temperature would increase or decrease the overall performance of the filter.

References

1. S. Kawatsu, *J. Power Sources*, **71**, 150 (1998).
2. T. Zawodzinski, T. Springer, J. Bauman, T. Rockward, F. Uribe, and S. Gottesfeld, in *Proton Conducting Membrane Fuel Cells II*, S. Gottesfield and T. F. Fuller, Editors, PV 98-27, p. 127, The Electrochemical Society Proceedings Series, Pennington, NJ (1998).
3. J. H. Hirchenhofer, D. B. Stauffer, R. R. Engleman, and M. G. Klett, *Fuel Cell Handbook*, 4th ed., p. 7-3, Parsons Corporation, Reading, PA (1998).
4. H. P. Dhar, L. G. Christner, A. K. Kush, and H. C. Maru, *J. Electrochem. Soc.*, **133**, 1574 (1986).
5. H. F. Oetjen, V. M. Schmidt, U. Stimming, and F. Trila, *J. Electrochem. Soc.*, **143**, 3838 (1996).
6. H. P. Dhar, L. G. Christner, and A. K. Kush, *J. Electrochem. Soc.*, **146**, 1613 (1999).
7. H. Kita, S. Ye, and K. Sugimura, *J. Electroanal. Chem. Interfacial Electrochem.*, **297**, 283 (1991).
8. E. J. Carlson, A. J. Mariano, S. Hynek, S. Sriramulu, and G. Stevens, Cost analysis of fuel cell system for transportation application: final report to DOE (2000).
9. F. R. Preli, in *Fuel Cell Technology: Opportunities and Challenges*, AIChE Spring Topical Conference Proceedings, p. 12 (2002).
10. C. D. Dudfield, R. Chen, and P. L. Adcock, *J. Power Sources,* **85**, 237 (2000).
11. C. D. Dufield, R. Chen, and P. L. Adcock, *Int. J. Hydrogen Energy*, **26**, 763 (2001).
12. M. S. Wilson, U.S. Pat. 5,211,984 (1993).
13. R. J. Bellows, E. P. Marucchi-Soos, and D. T. Buckley, *Ind. Eng. Chem. Res.,* **35**, 1235 (1996).
14. M. Metikos-Hukovic and S. Omanovic, *J. Mol. Catal. A: Chem.*, **136**, 75 (1998).
15. H. A. Gasteiger, N. Markovic, and P. N. Ross, *J. Phys. Chem.*, **99**, 8290 (1995).
16. H. A. Gasteiger, N. Markovic, P. N. Ross, and E. J. Cairns, *J. Phys. Chem.*, **98**, 617 (1994).